Journal of Cellular Biochemistry 94:336–350 (2005)

Suppression of Cyclic GMP-Specific Phosphodiesterase 5 Promotes Apoptosis and Inhibits Growth in HT29 Cells

Bing Zhu, Lakshmi Vemavarapu, W. Joseph Thompson, and Samuel J. Strada*

Department of Pharmacology, University of South Alabama College of Medicine, Mobile, Alabama 36688

Abstract Phosphodiesterase 5 (PDE5) is a major isoform of cGMP phosphodiesterase in a variety of human tumor cell lines and plays a key role in regulating intracellular cGMP concentrations ($[cGMP]_i$). Here, we demonstrate that suppression of PDE5 gene expression by antisense *pZeoSV2/ASP5* plasmid transfection results in a sustained increase in $[cGMP]_i$, growth inhibition, and apoptosis in human colon tumor HT29 cells. With stable transfection, antisense transcripts exhibited a specific suppression in PDE5 activity, mRNA levels, and a 93 kDa *h*PDE5A1 protein. In cloned antisense cells, prolongation of the cell growth doubling times correlate positively with suppressed PDE5 activity and increased $[cGMP]_i$. The growth inhibition in PDE5 antisense clones is due to an increased apoptotic rate and delayed cell-cycle progression. These results corroborate previous findings with the PDE5 inhibitor exisulind and its derivatives showing that sustained $[cGMP]_i$ induces apoptosis and growth inhibition in tumor cells. Furthermore, an inducible mitotic inhibitor $p21^{WAF1/CIP1}$ has been found to account for the delay of cell-cycle progression in PDE5 antisense clones at G_2/M phase. A proteolytic cleavage of $p21^{WAF1/CIP1}$ in the antisense clones is also increased at the later stage of serum stimulation. The protein kinase G (PKG) inhibitor, KT5823, can prevent the cleavage of $p21^{WAF1/CIP}$. These data substantiate a pivotal role for PDE5 as a modulator of apoptosis and cell-cycle progression for human carcinoma via a mechanism involving the activation of $[cGMP]_i$/PKG signaling pathways. J. Cell. Biochem. 94: 336–350, 2005.

Key words: phosphodiesterase; antisense; cGMP; apoptosis; growth inhibition; HT29; $p21^{WAF1/CIP1}$

Phosphodiesterase 5 (PDE5) is one member of several cyclic nucleotide phoshodiesterase gene families that hydrolyze cyclic GMP (cGMP-PDEs) [Fawcett et al., 2000; Francis et al., 2000; Soderling and Beavo, 2000]. The enzyme activity of PDE5 is characterized by cGMP-specific hydrolysis and cGMP-binding capability. PDE5 regulates the basal levels and intensity and duration of guanylyl cyclase (GC) agonist-induced changes of intracellular cGMP concentration $[cGMP]_i$ in normal and abnormal cells. An up-regulated PDE5 expression was recently shown in multiple human carcinoma and neoplasm and animal tumorigenesis as compared with the normal counterpart tissues. For example, increased amounts and activities of PDE5 were detected in human transitional and squamous cell carcinoma of neoplastic bladder versus normal urothelium [Piazza et al., 2001], and specimens of human colonic neoplasias with familial adenomatous polyposis (FAP) versus normal mucosa [Piazza et al., 2000]. PDE5 was also detected as a predominant isoform of cGMP-PDEs in many carcinoma cell lines in culture, including colonic adenocarcinoma (SW480, HCT116, HT29, T84), breast cancer (HTB-26, MCF-7), lung cancer, bladder, and prostate cancer (LNCAP, PC3), and leukemia [Thompson et al., 2000; Whitehead et al., 2003]. In the aggregate, these studies point towards a functional role of an up-regulated PDE5 enzyme in controlling cellular pathways involved in carcinoma cell growth.

Abbreviations used: $[cGMP]_i$, intracellular cGMP concentrations; cGMP PDE, guanosine 3′,5′-cyclic monophosphate phosphodiesterase; PDE5, phosphodiesterase 5; $T_{1/2}$, growth doubling time; PKG, protein kinase G.

*Correspondence to: Samuel J. Strada, University of South Alabama College of Medicine, CSAB 170, Mobile, AL 36688. E-mail: sstrada@usouthal.edu

Received 7 April 2004; Accepted 19 July 2004

DOI 10.1002/jcb.20286

Direct evidence for PDE5 involvement in regulating tumor cell growth and death comes from studies of the pre-apoptotic and growth inhibitory effects of sustained $[cGMP]_i$. Increased $[cGMP]_i$ elicited by various GC-agonists, for example, guanylin/uroguanylin [Shailubhai et al., 2000], atrial natriuretic peptide [Wu et al., 1997], YC-1 [Thompson et al., 2000], nitric oxide donors [Guh et al., 1998], and/or PDE5-selective inhibitors, for example, sildenafil and vardenafil [Sarfati et al., 2003], induce apoptosis and anti-proliferation. Moreover, the inhibition of cGMP hydrolytic activity by selective inhibitors of PDE5 not only potentiates the effects of GC agonists but also maintains a persistent increase in $[cGMP]_i$, as opposed to a transient increase in $[cGMP]_i$ when the PDE5 activity is present. This concept is further supported by a study with a novel class of PDE5 inhibitors, exisulind (sulindac sulfone) and its higher affinity analogues. These drugs induce apoptosis and inhibit cell proliferation in colonic tumor cell lines via a mechanism of cellular signal transduction that involves persistent increases in $[cGMP]_i$ and down-stream targets [Thompson et al., 2000]. A strong correlation was noted in rank order potencies for PDE5 inhibition and apoptosis. Preliminary clinical studies with these exisulind derivatives have shown promising results in some cancer patients suggesting novel targets for cancer chemotherapy [Chan et al., 2002; Dy and Adjei, 2002; Sun et al., 2002]. Thus, PDE5 inhibition appears essential for controlling sustained $[cGMP]_i$-mediated apoptosis and anti-proliferation in carcinomas.

To further substantiate the role of PDE5 expression in controlling carcinoma growth and death, here we demonstrate a suppression of PDE5 expression in human colonic tumor HT29 cells using an antisense approach. Regulatory domains of human *PDE5A1/A2* genes have been partially cloned from HT29 cells [Liu et al., 2002] and show a close identity to the cloned human *PDE5A* genes [Lin et al., 2000a,b]. The PDE5 enzyme activity has also been identified as the predominant cGMP hydrolytic activity present in HT29 cells. A constructed antisense RNA expression vector, which carries a human PDE5A-specific cDNA domain in protein kinase G (PKG)-phosphorylation sites, has been used in the current study to suppress the PDE5 expression and induce the predicted effects on cell growth and apoptosis.

MATERIALS AND METHODS

General Materials and Reagents

[2,8-^{3}H] cyclic AMP and [8-^{3}H] cyclic GMP (Moravek Biochemicals, Inc., Brea, CA) and Dowex-1X8-400 resin (Sigma, St. Louis, MO) were prepared as described previously [Thompson et al., 1979]. Proteinase inhibitors (benzamidine, TLCK, aprotinin, pepstain A, and leupeptin) and snake venom were from Sigma. PDE isoform-selective inhibitors: zaprinast (PDE5/6), rolipram (PDE4), cilostamide (PDE3), EHNA (PDE2), and vinpocetine (PDE1) were obtained from Calbiochem (La Jolla, CA). The kinase agonist, 8-Br-cGMP, and inhibitors, KT5823 and KT5720, were purchased from Calbiochem.

Cell Culture

Human colon adenocarcinoma HT29 cells were obtained from the American Type Culture Collection (Rockville, MD) and grown under 5% CO_2 at 37°C in RPMI-1640 medium with 5% FBS and 1% penicillin/streptomycin.

Plasmid Constructs

For antisense use, a 321 bp cDNA (*ASP5*) encoding the phosphorylation domain for human PDE5A1 (A2) was amplified by RT-PCR using total RNA isolated from HT29 cell (Fig. 1). The sequence of *ASP5* was further confirmed for its identity to a part of the amino terminal regulatory domain of *h*PDE5A1 (136–1,617 bp) as previously cloned from the same HT29 cell line [Liu et al., 2002] and was listed in GeneBank. Specific primers for *ASP5* were 5′-GGGCCCTGTTAGAAAAGCCACCAG-3′ and 5′-GGTACCGAGTCTTGAGCACTGGTC-3′. *ASP5* was ligated to produce an expression plasmid *pZeoSV2/ASP5* with an antisense reading frame orientation under SV40 promoter and *zeocine* resistance. Plasmid *pZeoSV2/ASP5* or β-galactosidase control plasmid *pZeoSV2/lacZ* were amplified in Top10 *E. coli* strain. All reagents were from Invitrogen (Carlsbad, CA).

Antisense Transfection and Stable Cell Line Selection

Ten micrograms of linearized plasmid was electroporated into HT29 cells in a FBS free RPMI-1640 medium along with mock transfection. *Zeocine* at 0.3 mg/ml (5× TC_{50} for HT29 cells) was added to select resistant cells with stable transfection. After 4 weeks in culture,

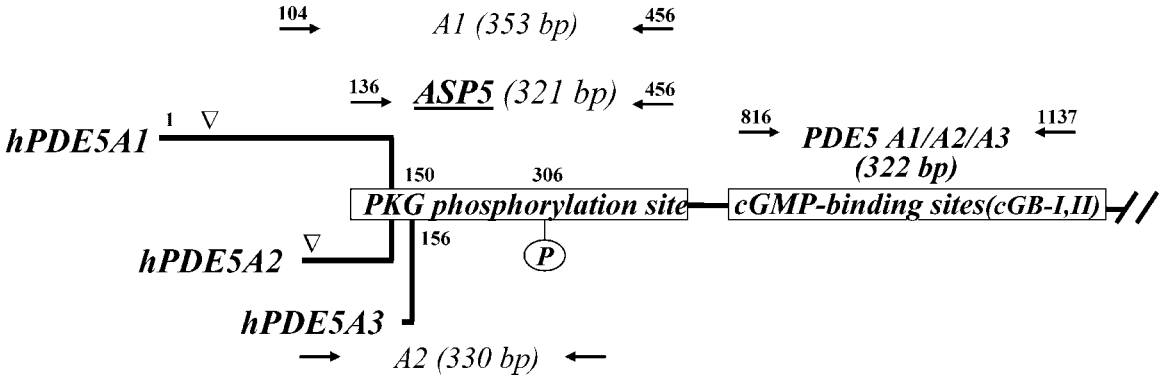

Fig. 1. Schema of target human PDE5 antisense cDNA for vector construct. A 321 bp PDE5-specific cDNA (*ASP5*) covering PKG-phosphorylation site of *hPDE5A1*(*A2*) was constructed as a 3.8 kb *pZeoSV2/ASP5* plasmid with antisense reading orientation under SV40 promoter and *zeocine* resistance. Regulatory domains of human PDE5A1/A2 genes were cloned from colonic tumor HT29 cells. Arrows indicate the primers used for PDE5 antisense cDNA cloning and RT-PCR to detect mRNA for A1/A2/A3 (322 bp), A1 (353 bp), and A2 (330 bp). The ''∇'' symbols indicate the relative domains of antibodies raised for A1 and A2 splice variants.

isolated colonies from antisense and *LacZ* transfected cells were harvested for PDE activity assay and all cells in mock transfection were dead by *zeocine* selection. One of the antisense colonies, *ASC4*, was further sub-cultured by limited dilution (one cell per 3-wells in 96-wells plate) to achieve single cell clones. All transfected cells were maintained in *zeocine* medium (0.06 mg/ml) with passages every 5 days and kept in culture within 50 days for further tests. PDE activities in cell supernatants were measured with 0.25 μM ^{3}H-cGMP or ^{3}H-cAMP as substrate [Thompson et al., 2000].

Relative Quantitative (RQ) RT-PCR

RQ RT-PCR was performed according to *QuantumRNA 18S Internal Standards* Competimers techniques (Ambion, Austin, TX) with total RNA extracted by *RNA* isolation kit (Roche, Indianapolis, IN) and cDNA prepared by *First Strand RT-PCR* kit (Stratagene, La Jolla, CA) with random primers. Primers for human PDE5 (A1, A2, and A3) are: 5′-GAATCATAGGGAAGAGGTTGTTGG-3′ and 5′-AGAATCGGAGCAATCTTCATCCAC-3′ to produce a 322 bp band (Fig. 1) versus internal control 18S RNA at 488 bp. Primers for human PDE4A (5′-TACGCTGGAGGCCGCTCACTC-3′ and 5′-GCTGAGGTTCTGGAAGATGTCGCAG-3′) produced a band at 426 bp that was used as a native PDE isoform mRNA control in RQ RT-PCR.

Western Blot Analysis

Whole cell extraction and immunoblotting was performed as described previously [Thompson et al., 2000]. Antibody to GST-fusion protein of the high affinity cGMP-binding domain of human PDE5 (cGB-I) [Liu et al., 2002] was prepared to recognize the PDE5 A1/A2/A3 variants. The N-terminal peptides (Fig. 1) were used to develop specific antibodies for PDE5 A1 (CMERAGPSFGQQRQQQQPQQQ) and A2 (CMLPFGDKTR). Antibody to PDE4A was prepared as previously described [Thompson et al., 2002]. Goat IgG to the N-terminal peptide of human PDE3B (RGFFFHLCRFCNVE) was also prepared and affinity-purified (Bethyl Laboratories, Montgomery, TX) and compared with PDE3B (N-20) antibody purchased from Santa Cruz Biotechnology (Santa Cruz, CA). Rabbit polyclonal antibody (H-164) raised against recombinant protein corresponding to amino acids 1–164 of full length $p21^{WAF1/CIP1}$ of human origin and antibody raised against a peptide mapping at the carboxy terminus of human origin (C-19) were obtained from Santa Cruz. These antibodies were used to detect either full length $p21^{WAF1/CIP1}$ (H-164) or full length plus cleaved $p21^{WAF1/CIP1}$ (C-19). Anti-human $p27^{KIP1}$ and p14ARF/p16INK4a (Santa Cruz), cyclin A, B1, and D1/D2 (Upstate, Lake Placid, NY), cdk2 and cdc2 (Stressgen, Victoria, Canada) antibodies were also used in immunoblots.

EIA for $[cGMP]_i$ and $[cAMP]_i$

The whole cell acid extracts in 0.2 N HCl/50% methanol were prepared as described previously [Thompson et al., 2000]. The amount of cGMP and cAMP in acetylated samples were

measured using enzyme immunoassay (EIA) kits (Cayman Chemical, Ann Arbor, MI). Data were expressed as pmol of $[cGMP]_i$ and $[cAMP]_i$ generated per milligram total protein of the cells.

DNA Fragmentation and Cell Growth Curves

DNA fragmentation in control *LacZ* and antisense cells in 96-wells plate was measured using a DNA/histone-complex ELISA kit (Roche) as described [Thompson et al., 2000]. Comparative values of DNA fragmentation among different cell lines were based on using the same cell number in each assay. Cell proliferation was determined by MTT assay as described [Guh et al., 1998]. Growth curves and doubling times were plotted and calculated by *GrapghPad Prism* software.

Immunofluorescence

Histochoice (Amresco, Solon, OH) fixed cells were permeabilized with 0.5% Triton X-100 in PBS and incubated with anti-PDE5 and/or M30 CytoDeath antibody binding to a caspase cleaved cytokeratin-18 to indicate cell apoptosis (Roche). Cells were incubated with secondary antibodies conjugated with Cy3 (Jackson ImmunoResearch Laboratories, West Grove, PA) or FITC (SouthernBiotech, Birmingham, AL) and observed using confocal fluorescence microscope (Leica, TCS SP2).

Serum-Deprived Synchronized Flow Cytometry

Cells were plated in 5% FBS medium for 7 days until 90% confluent and the medium was changed to 0.2% FBS for another 3 days to achieve serum-deprived cell synchronization at G_0/G_1 phase [Tobey et al., 1988; Dietrich et al., 1997; Davis et al., 2001]. Cells were re-seeded to 5% FBS medium for the times indicated. DNA content was measured with FACS-scan (Becton Dickinson, SCANVantage SE) after cells were fixed in 70% ethanol and stained with 100 μg/ml propidium iodide to calculate cell-cycle distribution and apoptotic content using *CellQuest* software.

RESULTS

Antisense *pZeoSV2/ASP5* Stably Suppressed PDE5 Expression at Post-Transcriptional Levels

We have cloned regulatory domains of *PDE5* genes from a human colonic tumor HT29 cell line [Liu et al., 2002] and verified that the sequence of such domains is identical to the human *PDE5A* genes which were previously reported as three splice variants A1, A2, and A3 in human, rat, and bovine tissues (Fig. 1) [Lin et al., 2000b]. Although message RNAs for PDEs 1–11 are detectable using RT-PCR methods, significant amounts of measurable cyclic nucleotide hydrolysis in HT29 are restricted to isoforms of only three PDE gene families: PDE 5, 4, and 3 (Table I).

TABLE I. Summary of PDEs Isotype Expression in Human Colon Tumor HT29 Cells

PDE family	mRNA (subtype)[a]	Activity and amount (inhibitor)[b]	DEAE column (Elution peak)[c]	Immuno-reactivity (Western blot)[d]	Subcellular location (immunofluorescence)[e]
PDE1–2	+	N.D.	N.D.	—	—
PDE3	+ (*3A*/*3B*)	+, Minor (Cilostamide)	cAMP/cGMP (500 mM NaAC)	3B: 140 kDa 3A: N.D.	Membrane
PDE4	+ (A–D)	+, Major (Rolipram)	cAMP (500 mM NaAC)	4A: 87 kDa 4B–D: N.D.	Cytoplasm
PDE5	+ (A1 > A2)	+, Major (Zaprinast)	cGMP (110 mM NaAC)	5A1: 93 kDa 5A2: 85 kDa	Cytoplasm
PDE6–11	+	N.D.	N.D.	—	—

N.D., not detected;—, not determined, PDE, phosphodiesterase.
[a]Detected by RT-PCR using total isolated RNA and PDE isoform- and correlated splice variants-specific primers. For PDE5, the amplified PCR product for 5A1 was detected higher than 5A2 (A1 > A2) based on the same amount of total RNA.
[b]PDE isoform-selective inhibitors including zaprinast (PDE5), rolipram (PDE4), and cilostamide (PDE3) were used to confirm isoform-specific cAMP and cGMP-hydrolytic activities in HT29 cells either by whole cell extractions or partial purification with DEAE chromatography. Other PDE inhibitors used in the studies were listed in Materials and Methods.
[c]DEAE-TM chromatography were used to isolate and quantitate relative amounts of the PDE isoforms present in whole cell extracts in 1% Trition X-100 as previously described [Thompson et al., 2000]. PDE activities were measured in fractions eluted by linear concentrations (0–1,000 mM) of NaAC and further characterized using the selective inhibitors. One major cGMP-hydrolytic peak was identified as eluting at low salt concentration (110 mM NaAC) and characterized as PDE5. Another minor cGMP-hydrolytic peak (PDE3) was found at high salt elution (500 mM NaAC). Only one cAMP-hydrolytic peak was found at 500 mM NaAC that consisted of a mixture of activities, PDE4 (major) and PDE3 (minor).
[d]Antibodies against PDE5, 4, and 3 and correlated splice variants were raised and used as described in Materials and Methods. The major PDE isofoms in HT29 cells (PDE5A1 and PDE4A) are underlined.
[e]The antibodies used for immunocytochemistry were the same as those used in Western blot.

PDE5 accounts for more than 95% of the cytoplasmic and approximately 85% of the whole cell cGMP hydrolysis, with a minor activity from PDE3B (140 kDa) activity associated with particulate fractions (Table I). A comparable percent of cytoplasmic cAMP hydrolysis from PDE4A (87 kDa) is detectable, with a smaller amount from PDE3B. The major immunoreactivity of a 93 kDa PDE5 was detected with an antibody recognizing all spliced variants of *hPDE5A1/A2/A3* genes, and was subsequently identified as *h*PDE5A1 (875 amino acid) with a 5A1-specific antibody. Only a trace level of a 85 kDa protein indicating the presence of *h*PDE5A2 was detected by a 5A2-specific antibody. RT-PCR and immunoprecipitation confirmed the ratio of dominant *h*PDE5A1/A2 variants in HT29 cells with a lesser amount of 5A2 than 5A1 and the absence of any truncated 5A3 expression. Thus, the 93 kDa *h*PDE5A1 is the major cytosolic cGMP hydrolytic activity present in cultured HT29 cells. These results are similar to what have been found in other colonic tumor cells [Thompson et al., 2000]. Immunofluorescence studies showed a subcellular locale for PDE5 that is primarily in discrete perinuclear foci (refer to Fig. 5A), which is also similar to observations seen previously in bladder tumor cells [Piazza et al., 2001].

To construct an antisense cDNA expression vector, a 321 bp cDNA (*ASP5*) containing the PKG phosphorylation domain of PDE5 A1 and A2 was ligated to a *pZeoSV2*(+) vector with an SV40 promoter. After electroporating the linearized *pZeoSV2/ASP5* plasmid to HT29 cells and 4 weeks of selective culture in *zeocine*, we obtained 15 cell colonies from antisense stable transfection, termed *ASA3-ASD6*. Ten other colonies, termed *LacZ*, with introduced β-galactosidase activity were obtained from control vector *pZeoSV2/LacZ* transfection. Twelve antisense colonies cells showed variable 25–70% reductions of PDE5 activity versus the *LacZ* control and the un-transfected HT29 cells. One of the antisense colonies cells, *ASC4* (Fig. 2A), showed the most inhibition (>70%) in cytosolic cGMP hydrolytic activity (specific activity = 13.8 ± 0.5 pmol/min/mg protein in HT29 cell). Conversely, all antisense colonies have no significant change in the activities of cytosolic cAMP hydrolysis as compared to each other or to control cells (specific activity = 49.2 ± 0.7 pmol/min/mg protein in HT29 cell).

Using limited dilution of cell culture, 12 descendant clones (*S4-S34*) were obtained from the original *ASC4* cells. Seven clones showed more PDE5 suppression than their parent *ASC4*, while the others showed a similar or less inhibition (Fig. 2A). These results suggest that *ASC4* is composed of various cell clones having different expressions of PDE5 antisense RNA transcripts. One of the clones, *S16*, showed the most significant inhibition, i.e., inhibition of about 92% in PDE5 activity ($P < 0.01$ vs. *LacZ* control). In addition, unchanged activities of PDE4 or PDE3 were found in these clones indicating a selective inhibition of PDE5 expression by the antisense construct.

RQ RT-PCR indicated that the down-regulated expression of PDE5 in antisense cells was specific to mRNA blocking. At the same levels of 18S RNA, PDE5 mRNA decreased in the antisense cells without changing the level of PDE4 transcription (Fig. 2B). Western blots showed a specific decrease of the 93 kDa PDE5A1 immunoreactivities in antisense clones, and no alteration in the 87 kDa PDE4A (Fig. 2C). A strong correlation exists between the levels of decreased PDE5 activities, mRNA, and protein in the antisense transfected clones (data not shown). PDE profiles in DEAE chromatography showed a reduction of PDE5 activity to 85% in *S16* cells as compared with *LacZ* control cells, without changes in PDE4 and PDE3 activities or the appearance of any novel PDE isoforms (data not shown). The duration of reduced PDE5 activity in a continuously cultured *S16* clone was maintained for up to 75 days with the activity gradually returning to pre-transfection levels at about 200 days, perhaps reflecting a relapse of antisense expression.

Increased Intracellular Cyclic Nucleotide Content by PDE5 Suppression

The level of $[cGMP]_i$ in cultured HT29 cells is near 50 fmol/mg protein, whereas $[cAMP]_i$ is 100× higher, i.e., at 5,000 fmol/mg. These values are similar to those observed in other cultured colon tumor cell lines, for example, SW480 [Thompson et al., 2000]. There was no change of $[cGMP]_i$ or $[cAMP]_i$ in transfection control, *LacZ* cells.

The antisense clones that demonstrate significant suppression of PDE5 activities showed significant increases in $[cGMP]_i$ without changes in $[cAMP]_i$ (Fig. 3). The *S16* clone, in which the PDE5 activity was greatly inhibited, indicated the largest increases in $[cGMP]_i$. Further analysis using *GraphPad Prism* soft-

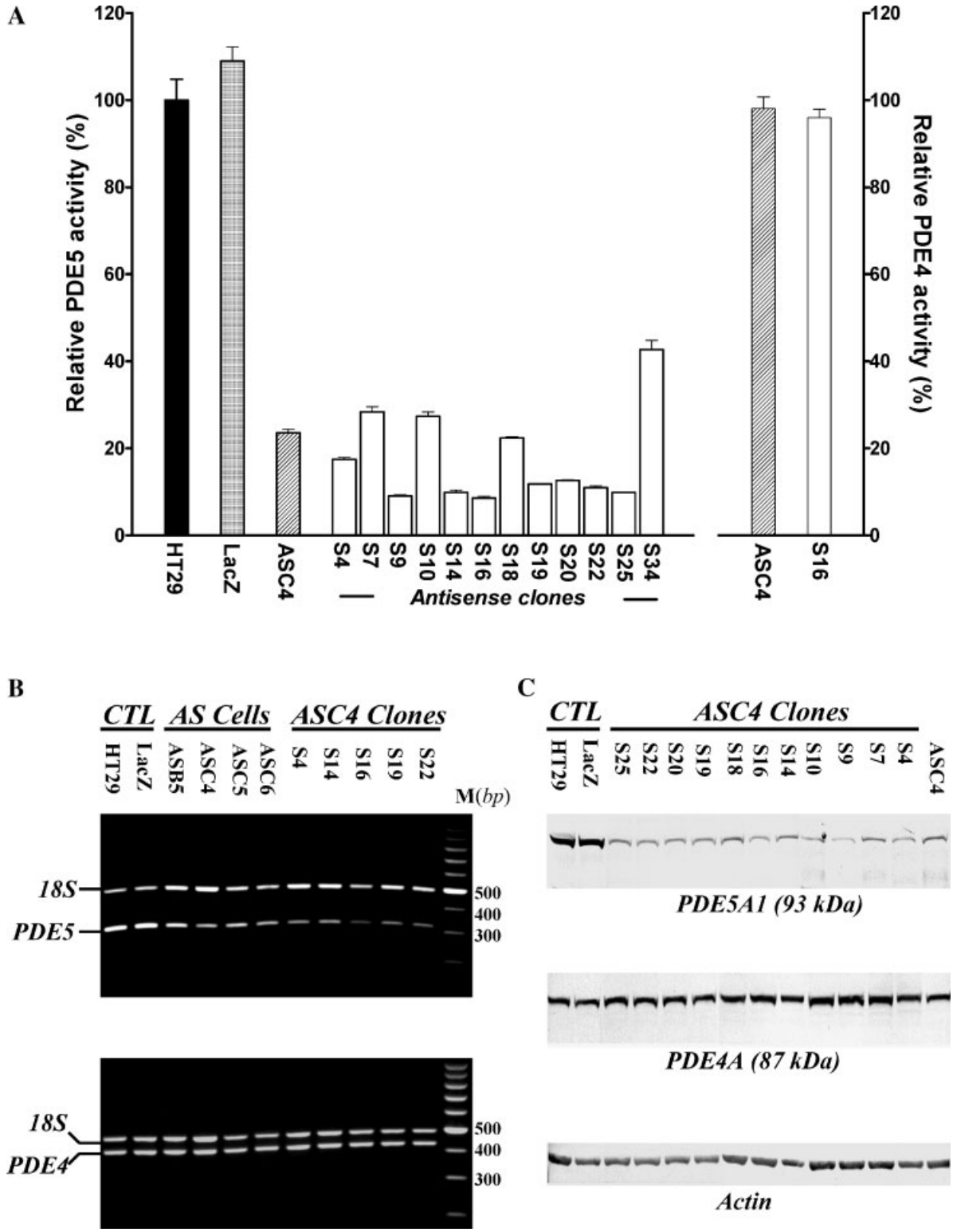

Fig. 2. Antisense selectively suppressed PDE5 expression in HT29 cells. **A**: PDE5 and PDE4 activities were measured in established *ASC4* antisense cells stably transfected with *pZeoSV2*/*ASP5* and descendent cells cloned from *ASC4* by limited dilution. The PDE5 cGMP-hydrolytic activities in the *ASC4* (up to 70% reduction) and clones (up to 92% reduction) are significantly lower than the activities in *pZeoSV2*/*LacZ* stable transfectants, *LacZ* controls, and un-transfected HT29 cells ($P < 0.05$, from six separated experiments), without changes in PDE4 cAMP-hydrolytic activities. The values for PDE5 and PDE4 specific activities in cytosolic extraction of HT29 cells are 13.8 ± 0.5 and 49.2 ± 0.7 pmol/min/mg protein, respectively. **B**: Relative quantitative (RQ) RT-PCR using 18S RNA/Competimers as internal control (488 bp) showing the down-regulation of PDE5 mRNA (322 bp) but not PDE4A (426 bp) in antisense cells (*AS*) and *ASC4* clones versus *LacZ* and HT29 controls (*CTL*). **C**: Immunoblots showing the down-regulation of PDE5 immunoreactivities at 93 kDa (5A1) but no change of PDE4A at 87 kDa in *ASC4* cells and descendent clones using actin (43 kDa) as the gel loading reference.

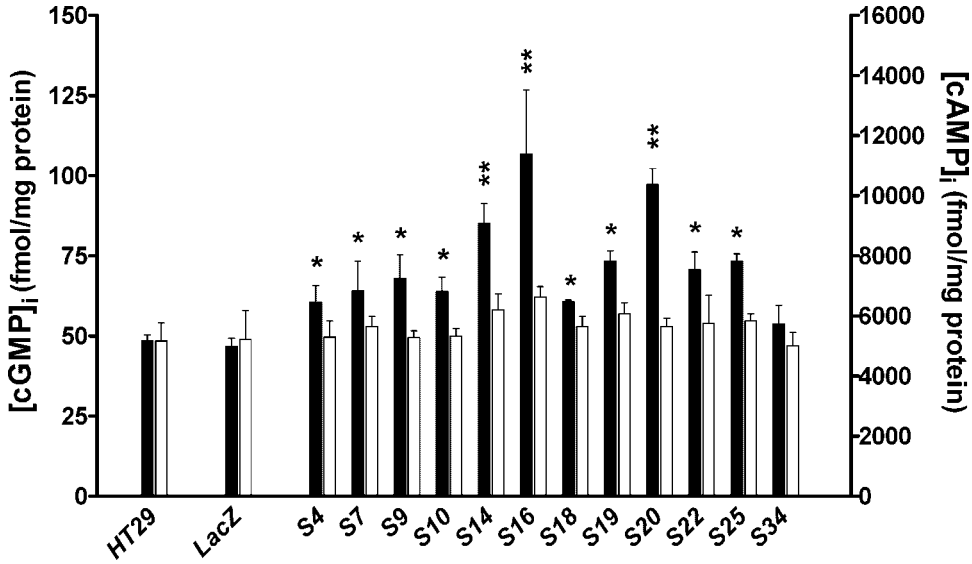

Fig. 3. Total intracellular cGMP concentration ($[cGMP]_i$) of antisense cells parallels suppression of PDE5. Increased $[cGMP]_i$ (solid bars) with constant $[cAMP]_i$ (open bars) in controls and total 12 antisense clones were determined by EIA assay. *, $P < 0.05$; **, $P < 0.01$ versus *LacZ* control, from five separated experiments.

ware demonstrates a one-phase exponential inverse correlation between reduced PDE5 activity and increased $[cGMP]_i$ among the 12 antisense clones (Fig. 4A). A relatively smaller increase in $[cGMP]_i$ occurs in those clones with a range of PDE5 suppression from 60 to 80%, but there are much greater increases in those clones with higher PDE5 inhibition (>90%). Therefore, a substantial inhibition of PDE5 expression by antisense appears essential to induce significant increases in $[cGMP]_i$ in HT29 cells.

Correlation of Growth Inhibition With Increased $[cGMP]_i$

Cloning of the antisense cells indicated that these cells had much slower growth rates than did the wild-type HT29 and *LacZ* controls in culture. When quantitated, the doubling times ($T_{1/2}$) for the antisense clones ranged from 27 to 45 h, whereas the doubling times for HT29 and *LacZ* cells were at 22 and 23 h, respectively. Growth inhibition in antisense clones also correlated with PDE5 suppression and $[cGMP]_i$ elevation. One phase exponential plots fit the data nicely for $[cGMP]_i$ versus $T_{1/2}$ in antisense clones (Fig. 4B) and PDE5 activities versus $T_{1/2}$ (data not shown). The data showed a near linear correlation between $[cGMP]_i$ and $T_{1/2}$ values in those clones where $[cGMP]_i$ increased from 50 to 75 fmol/mg protein and more growth inhibition in the clones with the "higher" $[cGMP]_i$ at 80–100 fmol/mg protein, such as *S14*, *S16*, and *S20*.

Increased Apoptosis and Delayed Cell-Cycle Progression by PDE5 Suppression

Cell cultures of antisense expressing cells showed increased apoptosis compared with vector control cells. When co-staining the cells with a PDE5-specific antibody and a M30-antibody against caspase-cleaved cytokeratin-18 [Leers et al., 1999; Kusama et al., 2000], confocal fluorescent images verified a correlation between PDE5 suppression and apoptosis in antisense *ASC4* cells (Fig. 5A). The staining of M30 with filamentous-type for early stage of apoptosis or granular-type for later stage of apoptosis co-localized only in those cells with weak or negative PDE5 staining. In addition, different densities (red) of PDE5 immunofluorescence in *ASC4* cells would be expected from the descendant clones with varying expression of PDE5 suppressed by antisense RNA transcripts (refer to Fig. 2). The *S16* clone showed similar M30 positive and PDE5 negative staining (data not shown). These morphological data were further confirmed with a higher "basal" apoptotic rate of DNA fragmentation in *S16* cells than *LacZ* controls and an increased apoptotic index after re-seeding *S16* cells to the culture plate at 48–96 h (Fig. 5B).

To further study the role of PDE5 in growth inhibition and cell-cycle progression, serum-

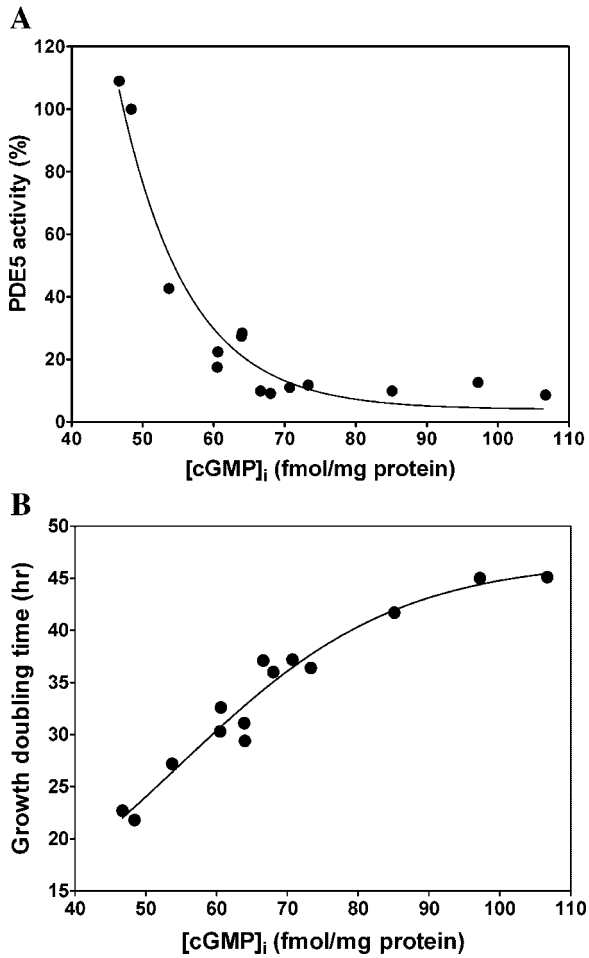

Fig. 4. Correlation of PDE5 inhibition, $[cGMP]_i$ elevation, and growth doubling time prolongation in HT29 cells with PDE5 suppression. Plots showing one-phase exponential inverse curve between $[cGMP]_i$ and PDE5 activity in 12 antisense clones and controls (**A**); and one-phase exponential associated curve between $[cGMP]_i$ and growth doubling time (**B**). The cell doubling time was obtained from the growth curves using the methods described in Materials and Methods. The values for PDE5 activity and $[cGMP]_i$ content were indicated in Figures 2 and 3.

deprivation was used as a method to synchronize the cells. After 72 h in 0.2% low serum medium and relatively high cell densities, FACS analysis showed a major population of cells synchronized at G_0/G_1 phase (>80%). When these cells were replenished with 5% serum, kinetics curves of cell phase distribution showed the time points of "*G_0/G_1-valley*," "*S-peak*," and "*G_2/M-peak*" for "synchronized" cell-cycle transition following serum re-stimulation. Time points of cell-cycle transition for HT29 and *lacZ* control were around 24 h whereas a significant delay was found in the antisense clones. Among them, *S16* cells showed a shift of the "*G_2/M-peak*" to 72 h (three times longer than control cells), and a similar but lesser amount of delay for "*S-peak*" or "*G_0/G_1-valley*" (Fig. 5C). Furthermore, the FACS analysis also showed that 5–30% cells were in sub-diploid apoptosis for antisense clones, whereas the index for control cells was below 1% under the same serum re-stimulation conditions (Fig. 5C). The maximum of the apoptotic index in FACS analysis was at 48–96 h after serum re-stimulation in the *S16* clone, also consistent with the DNA fragmentation data (Fig. 5B) measured at this time point.

Inducible $p21^{WAF1/CIP1}$ and Cyclin B1/A in Cell-Cycle Progression by PDE5 Suppression

To elucidate the mechanism for the delay of cell-cycle progression in PDE5 antisense cells, levels of cell-cycle specific molecules including cyclins, cdks, and cdk inhibitors (CKIs) were determined. After addition of 5% serum to re-stimulate synchronized cells, immunoreactivities of G_2/M phase specific cyclin B1 and $S–G_2/M$ phase-related cyclin A were increased in the antisense clone *S16* cells, either in initial *S16-1* (<7 days when colon cells established) or continuously cultured *S16-2* (7–45 days). At 72 h serum re-stimulation, both cyclin B1 and cyclin A were threefold higher in *S16* cells than in HT29 or *LacZ* control (Fig. 6A). A 50% increase of cyclin D2 (34 kDa) with no change in cyclin D1 (36 kDa) occurred in *S16* cells. No changes in cyclin dependent kinases including cyclin D related cdk2 and cyclin B1/A related cdc2 were detected in *S16* cells. A twofold to threefold increase of $p21^{WAF1/CIP1}$, the mitotic inhibitor, expression was found in *S16* cells as compared with control cells under the same condition of serum re-stimulation at 72 h (Fig. 6A). There were no changes in $p27^{KIP1}$, another mitotic inhibitor implicated in cyclin D1-cdk2, 4 and cyclin E-cdk2 inhibition at G_1 phase and inducible by TGFβ and increased $[cAMP]_i$ [Schreiber et al., 1999], nor was there a change in the inhibitors p14ARF/p16INK4a (data not shown).

Time courses of $p21^{WAF1/CIP1}$ expression in *S16-1* versus control *LacZ* were further studied at 0–96 h of serum re-stimulation (Fig. 6B). Both *LacZ* control and *S16* antisense cells showed a similar level of basal $p21^{WAF1/CIP1}$ expression in the serum-deprived cells (G_0/G_1 arrest). After serum replenishment, *LacZ* cells showed a decrease in $p21^{WAF1/CIP1}$ between 12 and 24 h with the lowest seen at 24 h (about 45%

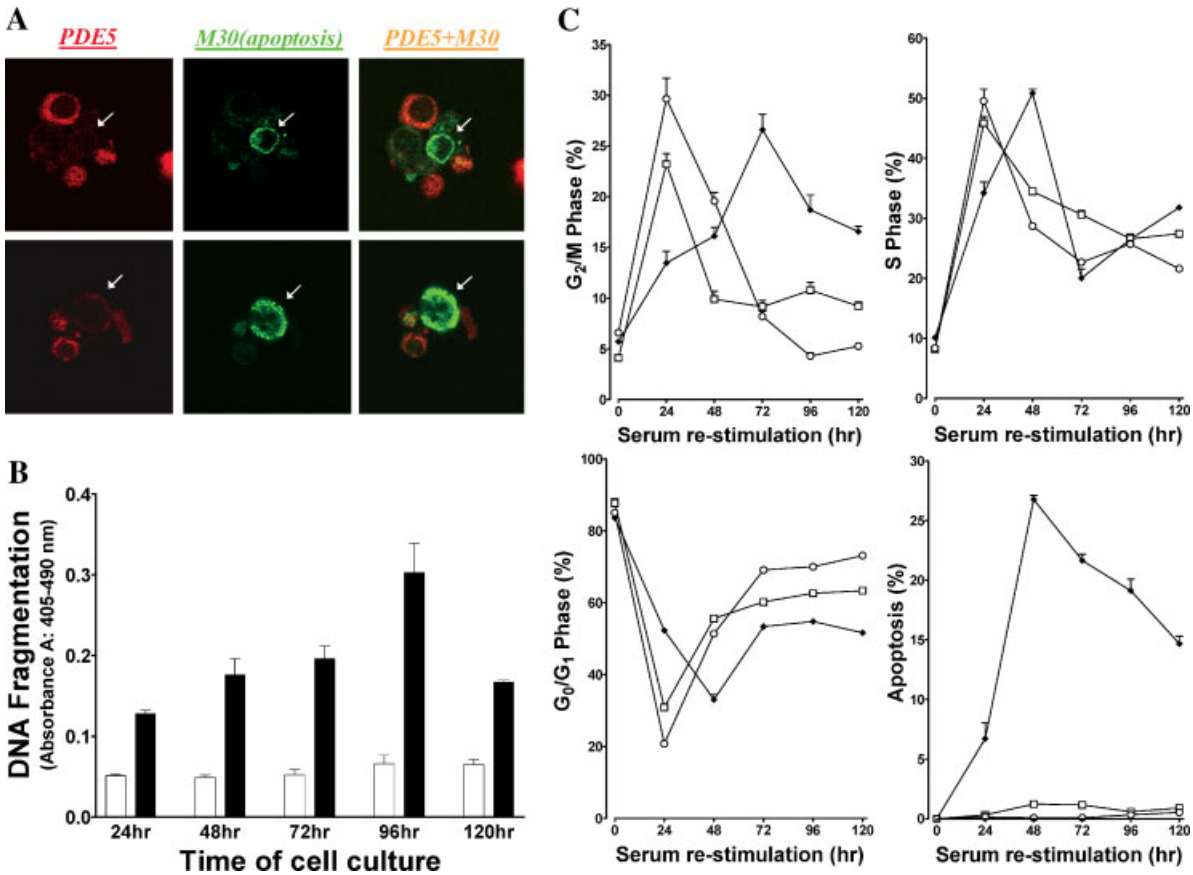

Fig. 5. Increased apoptosis and delayed cell-cycle progression by PDE5 suppression. **A**: Confocal immunofluorescence indicating PDE5 (red) by a PDE5 specific antibody and apoptosis (green) by a M30 antibody (caspase cleaved cytokeratin-18) in antisense *ASC4* cells. Arrows indicate cells in the process of early stage (**upper panel**, filamentous type) or late stage (**lower panel**, granular type) of apoptosis that co-localized with low or undetectable PDE5 staining (40×). **B**: Increased apoptosis determined with DNA fragmentation for endonuclease-cleaved mono- and oligo-nucleosomes (absorbance A at 405–490 nm) in antisense *S16* clone (solid bars) versus *LacZ* control (open bars). For comparative purposes, same amounts of cells (1,000 cell/20 μl cell lysis buffer) were used in the ELISA assay at the indicated time of cell culture. Data from one experiment repeated three times. **C**: FACS analysis showing cell-cycle progression at G_2/M, S, and G_0/G_1 phases and apoptotic indexes in serum re-stimulated synchronous antisense *S16* clone (◆) versus *LacZ* (□) and HT29 (○) controls. Data represent the average from three separated experiments.

of basal expression). Then, $p21^{WAF1/CIP1}$ returned gradually to the basal level after 24 h and kept the same level from 48 to 96 h in *LacZ* cells. These results suggest the role for basal level of $p21^{WAF1/CIP1}$ in controlling serum-stimulated normal cell-cycle transition from G_0/G_1 arrest to proliferation. There appears to be no further involvement of $p21^{WAF1/CIP1}$ at the later stage of cell proliferation with normal basal $[cGMP]_i$. Conversely, even though the expression of $p21^{WAF1/CIP1}$ in antisense *S16* cells and *LacZ* controls were similar during the first 12–24 h, a significant difference was found after 48 h. Indeed, an increased expression of $p21^{WAF1/CIP1}$ was found at 48 h, $147 \pm 16\%$ of basal ($P < 0.05$ vs. *Lac Z* control). This inducible $p21^{WAF1/CIP1}$ was maintained in *S16* from 72 ($182 \pm 16\%$) to 96 h ($252 \pm 32\%$), which was coincident with the time point of G_2/M phase delay (refer to Fig. 5C). In addition, changes of cyclin B1/A were also noted in *S16* cells under the same time course of serum re-stimulation and were comparable to $p21^{WAF1/CIP1}$ induction (Fig. 6B).

Proteolytic Cleavage of $p21^{WAF1/CIP1}$

Proteolytic cleavage of $p21^{WAF1/CIP1}$ has been found to play essential roles in tumor cell apoptosis and the process whereby cells convert from cell-cycle progression arrest to apoptosis [Jin et al., 2000; Kim et al., 2001; Ham et al., 2003]. We used an antibody (C-19) that can recognize both the full length of $p21^{WAF1/CIP1}$

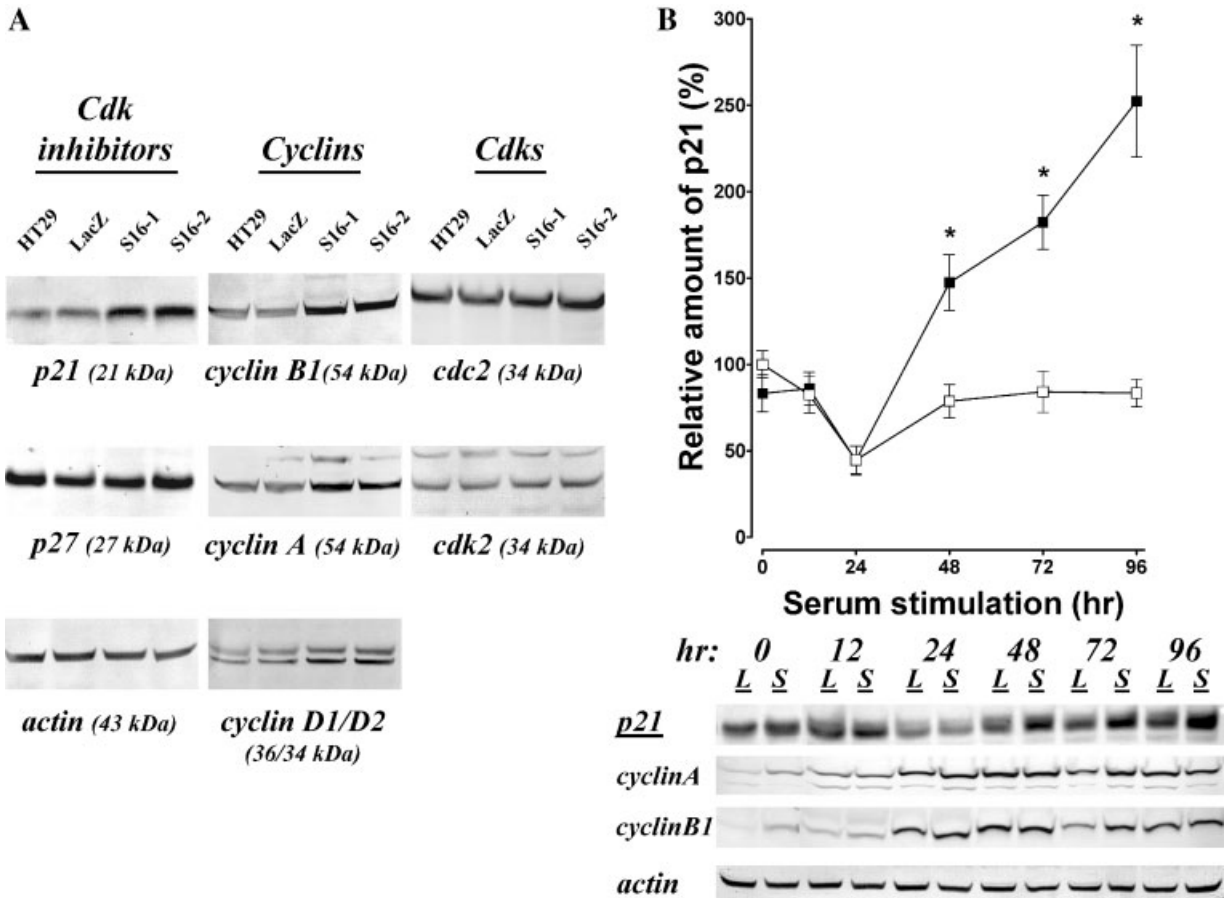

Fig. 6. Inducible expression of $p21^{WAF1/CIP1}$ and cyclin B1/A in antisense *S16* clone. *S16* cells in initial *S16-1* (<7 days) or continuously cultured *S16-2* (7–45 days) were synchronized to G_0/G_1 phase with serum-deprivation and then in cell proliferation induced by serum re-stimulation. One hundred micrograms of protein of whole cell extracts were loaded to 10% BT NuPAGE pre-cast gel. Immunoblots were performed as described in the legend of Figure 2C. All antibodies used in blots were obtained and used as described in Materials and Methods. **A**: Comparison of mitotic inhibitors ($p21^{WAF1/CIP1}$ and $p27^{KIP1}$), cyclins (A, B1, and D1/D2), cyclin dependent kinase (cdk2 and cdc2) expression in *S16* and control cells at 72 h of serum stimulation. Antibody (H-164), raised against human recombinant protein of $p21^{WAF1/CIP1}$, was used to detect full length of protein in Western blot. Representative results from one of three separate blots are shown. **B**: Time course for full length of $p21^{WAF1/CIP1}$ expression in *S16-1* (solid) and *LacZ* (open) cells from 0 to 96 h with serum stimulation indicating sustained inducible $p21^{WAF1/CIP1}$ expression in *S16* cells. After normalization to unstimulated *LacZ,* relative $p21^{WAF1/CIP1}$ immunoreactivties were plotted versus serum stimulation time. Data are expressed as average and standard error of six separate experiments that obtained and quantitated by densitometric scanning in *AlphaEase* software. *, $P < 0.05$ versus *LacZ* control at each point of time. Blots for $p21^{WAF1/CIP1}$, cyclin B1/A, and actin (protein amount control) at the bottom of the plot represent data from one experiment. ''*L*'' stands for *LacZ* control and ''*S*'' stands for *S16*.

(p21) and a cleaved fragment (p14) to distinguish changes in two polypeptides after serum re-stimulation. There was an increase of cleaved $p21^{WAF1/CIP1}$ fragment, with the full length one, in antisense *S16* cells versus *LacZ* control that occurred at 72–96 h of serum re-stimulation, but no such change was detected at the earlier stage of treatment (12–24 h, Fig. 7A). Furthermore, the PKG inhibitor, KT5823 (2 μM concentration which is 10× that of its K_i to inhibit PKG in vitro), blocked the increased cleavage of $p21^{WAF1/CIP1}$ in *S16* cells at 72 h but did not influence the level of full length protein (Fig. 7B). Neither the PKG agonist 8-Br-cGMP (5 μM) nor the PKA inhibitor KT5720 (1 μM concentration which is 10× that of its IC_{50} to inhibit PKA in vitro) influenced the cleavage of $p21^{WAF1/CIP1}$.

DISSCUSSION

PDE5 plays a key role in determining the sustained levels of $[cGMP]_i$ that impact cell growth and apoptosis in tumor cells. The

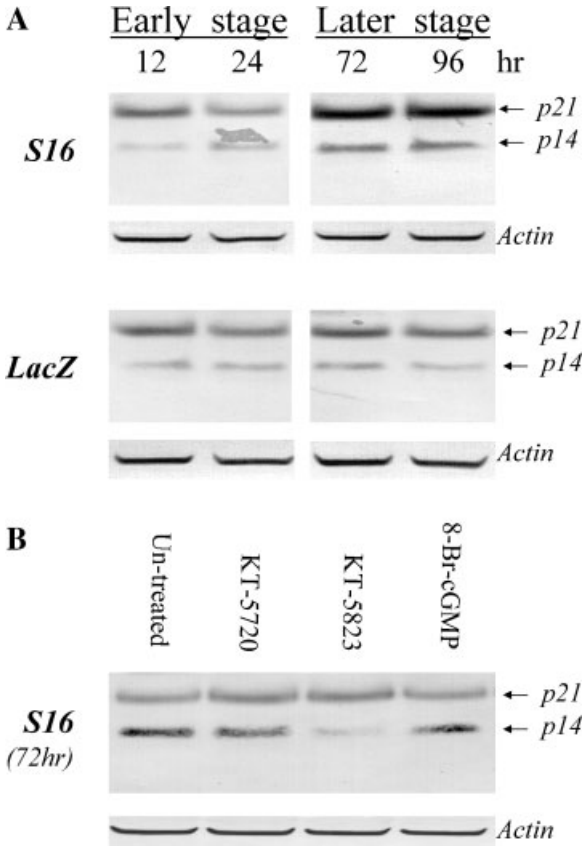

Fig. 7. A PKG-dependent proteolytic cleavage of $p21^{WAF1/CIP1}$ in the later stage of serum re-stimulation in antisense *S16* clone. Antibody (C-19) raised against carboxy terminus peptides of human $p21^{WAF1/CIP1}$ was used to detect both full length and cleaved proteins. **A**: Cleaved fragment, p14, for $p21^{WAF1/CIP1}$ was increased with full length of protein in *S16* cells in the later stage, 72–96 h, of serum re-stimulation, but not change in the early stage at 12–24 h versus control *LacZ* cell. **B**: The increased cleavage of $p21^{WAF1/CIP1}$ in *S16* cells was blocked by a treatment with PKG inhibitor, KT5823 (1 μM), at 72 h of serum re-stimulation. KT5823 showed no effect in the early stage at 24 h (data not shown). PKG agonist, 8-Br-cGMP (5 μM), did not further enhance the cleavage of under the same condition. PKA inhibitor, KT5720 (2 μM), showed no effect.

current study demonstrates that suppression of PDE5 expression in human HT29 cells via antisense vector *pZeoSV2/ASP5* transfection leads to sustained increases in $[cGMP]_i$, apoptosis, and growth inhibition. These data support the previous finding that inhibition of cGMP-PDE activities by exisulind and its higher affinity analogues induce apoptosis in colon tumor cells via persistent, rather than transient, elevations of $[cGMP]_i$ [Thompson et al., 2000]. A positive correlation between PDE5 suppression, $[cGMP]_i$ elevation, and growth inhibition has been shown in the antisense cells that have more than 90% of PDE5 activity suppressed in a specific manner without influencing other endogenous PDEs, for example, PDE4 and PDE3. This suggests that antisense RNA transcripts can be used effectively and with sequence specificity to influence post-transcriptional regulation of PDE5A gene expression in human tumor cells. It expands the number of studies that have used the antisense approach to suppress the expression of PDE genes [Jiang et al., 1996; Epstein, 1998; MacKenzie et al., 1998; Rybalkin et al., 2002]. Furthermore, the non-linear exponential correlation between PDE5 suppression and cGMP elevation in the various antisense clones indicates that a substantial and sustained suppression of PDE5 (>70%) is required to initiate a sustained $[cGMP]_i$ rise in these cells.

A quantitative correlation between $[cGMP]_i$ elevation and growth inhibition has been established, for the first time, with the reduction of PDE5 expression. Following the growth inhibition, increased apoptotic rates, measured by DNA fragmentation or apoptotic sub-diploid DNA in FACS analysis, also correlate quantitively with the increase in $[cGMP]_i$ and decrease in PDE5 expression under both basal culture and serum re-stimulation conditions. In addition, staining of caspase-cleaved cytokeratin 18 (M30) was detected in those antisense cells with very low or undetectable levels of PDE5 immunoreactivities. These results suggest that de-regulated PDE5 activity is critical to the proteolytic-mediated apoptosis as previously noted for exisulind derivatives [Thompson et al., 2000; Li et al., 2002]. A common or similar signaling mechanism for sustained $[cGMP]_i$-mediated apoptosis seems to exist in those tumor cells following the suppression of PDE5 expression by antisense and the inhibition of PDE5 activity by some selective pharmacological agents. Additional studies related to potential contributions of both GC and PDE5 isoforms to these complex processes are under investigation.

At least two novel downstream targets of activated protein kinase G (PKG) have been postulated to be involved in the process of PDE5/$[cGMP]_i$-mediated apoptosis in tumor cells. First, mutations of β-catenin and/or adenomatous polyposis coli (APC) in colon tumor cells lead to a defective phosphorylation of β-catenin by GSK3β kinase and β-catenin is unable to be degraded by ubiquitin-proteasomal. This situation

results in an accumulation of a cellular β-catenin pool that induces the abnormal tumor cell growth [Morin et al., 1997; Efstathiou et al., 1998; Hsi et al., 1999]. Attenuation of cellular β-catenin accumulation via a $[cGMP]_i$-activated PKG phosphorylation occurs in exisulind-treated colonic tumor cells that subsequently induces apoptosis [Thompson et al., 2000; Li et al., 2002]. Second, Soh et al. have reported that a phosphorylation and activation of MEKK1–SEK1–JNK1 pathway triggered by either exilulind-mediated PKG activation or a constitutively active mutant PKG construct promote cGMP-mediated apoptosis [Soh et al., 2000, 2001]. Since the mitogen-activated protein kinase family can respond to many external stress signals that could lead to the induction of apoptosis [Hochedlinger et al., 2002], activation of JNK1 by PKG and induction of apoptosis due to sustained $[cGMP]_i$ is implicated in PDE5 antisense cells as it occurs within the time course of serum-restimulation. A possible role for JNK1 activation in the apoptosis seen in PDE5 suppressed HT29 cells is also supported by the increase amounts of proteolytically cleaved $p21^{WAF1/CIP1}$ detected during the later stage of cell-cycle progression after serum restimulation (see below). In addition, certain growth factors that are involved in cell mitosis via their actions on the pool of cellular β-catenin [Davies et al., 2001] may also be influenced by PKG-mediated phosphorylation under the sustained $[cGMP]_i$ condition.

Delays in certain phases of cell-cycle transition with serum deprivation and replenishment appear to account for the prolongation of cell doubling time induced by PDE5 suppression. The delayed cell-cycle progression pattern in the PDE5 antisense HT29 cells did not show a phase-specific effect, as it involved the entire cycle from the G_0/G_1 phase to the G_2/M phase, however, with a larger delay occurring in the G_2/M phase. The exisulind derivatives, PDE5 inhibitor, does produce a more selective G_2/M arrest in tumor cells [Moon and Lerner, 2002; Yoon et al., 2002]. A delay of cell-cycle progression was also observed in T84 colonic tumor cells treated with the GC-C stimulator, uroguanylin [Pitari et al., 2001]. All these data suggest that the alteration of cell-cycle progression in these tumor cells is due to the increased cGMP-mediated signaling pathway.

The interplay of cyclin related proteins alters the speed or arrest of cell-cycle progression [Schreiber et al., 1999]. Changes in G_2/M phase related cyclin B1/A and, more importantly, inducible expression of mitotic inhibitor, $p21^{WAF1/CIP1}$, have now been identified in the PDE5 antisense cells. This finding suggests that after *PDE5* gene suppression a sustained $[cGMP]_i$-mediated G_2/M phase effect involves $p21^{WAF1/CIP1}$. The role of $p21^{WAF1/CIP1}$ is supposed to be specific at G_2/M phase with the cyclin B1/A, as it is found in mitosis inhibition [Bunz et al., 1998; Schmidt et al., 2001]. At least three lines of evidence support this hypothesis. First, serum-stimulated $p21^{WAF1/CIP1}$ induction in PDE5 antisense cells occurred at the later stages of cell proliferation (48–96 h), the time point when the cell-cycle progression was delayed at G_2/M phase; while *LacZ* control cells did not show this effect on $p21^{WAF1/CIP1}$. Second, G_2/M phase related cyclin B1 and A were induced at the same time period. Third, there was neither a significant change of G_0/G_1 phase specific cyclin D1/D2 nor the mitotic inhibitor $p27^{KIP1}$, which is known to affect G_1 phase cyclins/cdks and is inducible by $[cAMP]_i$/TGFβ [Schreiber et al., 1999; Schmidt et al., 2001]. These results suggest that the inducible $p21^{WAF1/CIP1}$ in PDE5 antisense cells leads to a cell-cycle progression delay mainly at the G_2/M phase with the interaction on cyclin B1/A-cdc2 complex rather than as a "universal" cdks inhibitor [Xiong et al., 1993]. Thus, we conclude that sustained $[cGMP]_i$ plays a unique role in regulating G_2/M phase-specific effects in HT29 cells via the regulation of $p21^{WAF1/CIP1}$. In addition, ERK1/2/MAPK maybe involved in cGMP-mediated induction of $p21^{WAF1/CIP1}$ [Gu et al., 2000] as depicted for PDE5 antisense HT29 cells in Figure 8.

A role for $p21^{WAF1/CIP1}$ in PDE5 suppressed HT29 cell appears to be involved in both the process of cell-cycle progression and also in the level of apoptosis seen in these cells. A coincidence of increased cleaved $p21^{WAF1/CIP1}$ with increased index of apoptosis occurs at the later stage of serum stimulation in PDE5 antisense cells. Recently, several studies have shown that a proteolytic cleavage of $p21^{WAF1/CIP1}$ by caspase-3 is required for ginsenoside-induced apoptosis in human hepatoma cells [Jin et al., 2000; Ham et al., 2003] and for TGF-β1-initiated conversion from a stage of cell-cycle progression arrest to apoptosis [Kim et al., 2001]. Indeed, these findings support the notion that proteolytic cleavage of $p21^{WAF1/CIP1}$ may affect the

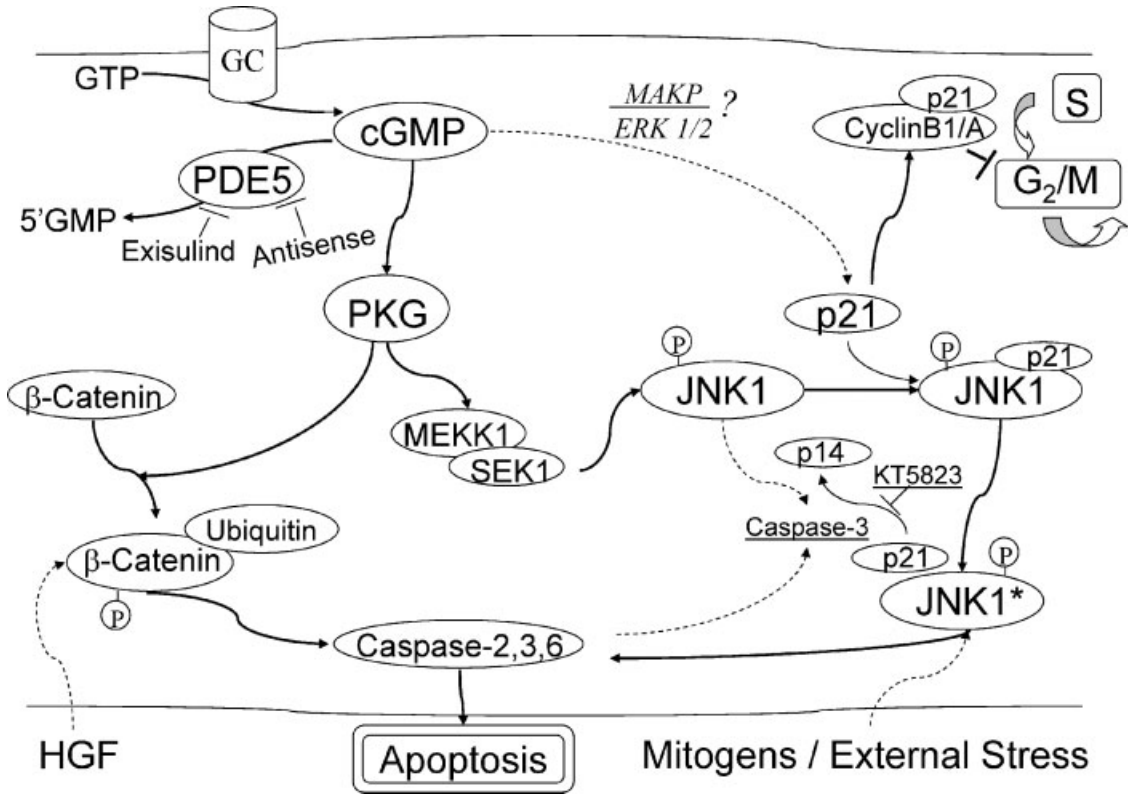

Fig. 8. Model depicting sustained $[cGMP]_i$-mediated apotptosis and interference of cell-cycle progression in tumor cell. A sustained increase in $[cGMP]_i$ occurs in tumor cells via the inhibition or suppression of dominant PDE5 activity in cGMP hydrolysis. Increased PKG activity by $[cGMP]_i$ activation mediates the phosphorylation of β-catenin and/or MEKK1-SEK1-JNK1 signaling pathways that lead to apoptosis. Under such conditions, an up-regulation of $p21^{WAF1/CIP1}$ and its proteolytic cleavage are involved in the regulation of cyclin B1/A-mediated cell-cycle progression and JNK1-activated apoptosis.

degree of apoptosis in PDE5 antisense HT29 cells. More importantly, we found that the increased cleavage of $p21^{WAF1/CIP1}$ in PDE5 antisense cells could be blocked by addition of the PKG inhibitor, KT5823, but not by a PKA inhibitor. Therefore, the proteolytic cleavage of $p21^{WAF1/CIP1}$ via a $[cGMP]_i$/PKG signaling pathway may be a primary mechanism involved in apoptosis in the PDE5 antisense HT29 cells (Fig. 8). In addition, the actions of JNK1 involve the cleavage of $p21^{WAF1/CIP1}$ to induce apoptosis in cancer cells [Ham et al., 2003]. Since exisulind induces apoptosis in colon cancer via a PKG–MEKK1–SEK1-mediated phosphorylation and activation in JNK1 [Soh et al., 2000, 2001], the role for JNK1 to induce apoptosis in PDE5 antisense transfected HT29 cells via a mechanism of PKG-mediated cleavage of $p21^{WAF1/CIP1}$ needs to be further studied.

In summary, a tight and specific correlation was established between PDE5, $[cGMP]_i$, and cell growth using a vector-based antisense cDNA to PDE5. In this regard, antisense RNA transcripts may serve as a useful approach to silence the over-expression of PDE5 in various tumors. The adaptive phenomenon of reduced PKG and $[cGMP]_i$, as observed in many tumor cells, may lead to the proapoptotic effects of increasing $[cGMP]_i$ in the cells. The antisense data in the present study implicate PDE5 as a potentially important endogenous modulator of apoptosis and cell-cycle progression in neoplastic cells and perhaps even in some normal cells.

REFERENCES

Bunz F, Dutriaux A, Lengauer C, Waldman T, Zhou S, Brown JP, Sedivy JM, Kinzler KW, Vogelstein B. 1998. Requirement for p53 and p21 to sustained G_2 arrest after DNA damage. Science 282:1497–1501.

Chan DC, Earle KA, Zhao TL, Helfrich B, Zeng C, Baron A, Whitehead CM, Piazza G, Pamukcu R, Thompson WJ, Alila H, Nelson P, Bunn PA, Jr. 2002. Exisulind in combination with docetaxel inhibits growth and metastasis of human lung cancer and prolongs survival in athymic nude rats with orthotopic tumors. Clin Cancer Res 8:904–912.

Davies G, Jiang WG, Mason MD. 2001. The interaction between β-catenin, GSK3β, and APC after motogen induced cell–cell dissociation, and their involvement in signal transduction pathways in prostate cancer. Int J Oncol 18:843–847.

Davis PK, Ho A, Dowdy SF. 2001. Biological methods for cell-cycle synchronization of mammalian cells. BioTechniques 30:1322–1331.

Dietrich C, Wallenfang K, Oesch F, Wieser R. 1997. Differences in the mechanisms of growth control in contact-inhibited and serum-deprived human fibroblasts. Oncogene 15:2743–2747.

Dy GK, Adjei AA. 2002. Novel targets for lung cancer therapy: Part II. J Clin Oncol 20:3016–3028.

Efstathiou JA, Noda M, Rowan A, Dixon C, Chinery R, Jawhari A, Hattori T, Wright NA, Bodmer WF, Pignatelli M. 1998. Intestinal trefoil factor controls the expression of the adenomatous polyposis coli-catenin and the E-cadherin–catenin complexes in human colon carcinoma cells. Proc Natl Acad Sci USA 95:3122–3127.

Epstein PM. 1998. Antisense inhibition of phosphodiesterase expression. Methods 14:21–33.

Fawcett L, Baxendale R, Stacey P, McGrouther C, Harrow I, Soderling S, Hetman J, Beavo JA, Phillips SC. 2000. Molecular cloning and characterization of a distinct human phosphodiesterase gene family: PDE11A. Proc Natl Acad Sci USA 97:3702–3707.

Francis SH, Turko IV, Corbin JD. 2000. Cyclic nucleotide phosphodiesterases: Relating structure and function. Prog Nucleic Acid Res Mol Biol 65:1–52.

Gu M, Lynch J, Brecher P. 2000. Nitric oxide increases $p21^{WAF1/CIP1}$ expression by a cGMP-dependent pathway that includes activation of extracellular signal-regulated kinase and p70(S6k). J Biol Chem 275:11389–11396.

Guh JH, Hwang TL, Ko FN, Chueh SC, Lai MK, Teng CM. 1998. Antiproliferative effect in human prostatic smooth muscle cells by nitric oxide donor. Mol Pharmacol 53: 467–474.

Ham YM, Choi JS, Chun KH, Joo SH, Lee SK. 2003. The c-Jun N-terminal kinase 1 activity is differentially regulated by specific mechanisms during apoptosis. J Biol Chem 278:50330–50337.

Hochedlinger K, Wagner EF, Sabapathy K. 2002. Differential effects of JNK1 and JNK2 on signal specific induction of apoptosis. Oncogene 21:2441–2445.

Hsi LC, Angerman-Stewart J, Eling TE. 1999. Introduction of full-length APC modulates cyclooxygenase-2 expression in HT-29 human colorectal carcinoma cells at the translational level. Carcinogenesis 20:2045–2049.

Jiang X, Li J, Paskind M, Epstein PM. 1996. Inhibition of calmodulin-dependent phosphodiesterase induces apoptosis in human leukemic cells. Proc Natl Acad Sci USA 93:11236–11241.

Jin YH, Yoo KJ, Lee YH, Lee SK. 2000. Caspase 3-mediated cleavage of $p21^{WAF1/CIP1}$ associated with the cyclin A-cyclin-dependent kinase 2 complex is a prerequisite for apoptosis in SK-HEP-1 cells. J Biol Chem 273:30256–30263.

Kim SG, Kim SN, Jong HS, Kim NK, Hong SH, Kim SJ, Bang YJ. 2001. Caspase-mediated Cdk2 activation is critical step to execute transforming growth factor-β1-induced apoptosis in human gastric cancer cells. Oncogene 20:1254–1265.

Kusama K, Jiang Y, Toguchi M, Ohno J, Shikata H, Sakashita H, Sakagami H. 2000. Use of the monoclonal antibody M30 for detecting HSG cell apoptosis. Anticancer Res 20:151–154.

Leers MP, Kolgen W, Bjorklund V, Bergman T, Tribbick G, Persson B, Bjorklund P, Ramaekers FC, Bjorklund B, Nap M, Jornvall H, Schutte B. 1999. Immunocytochemical detection and mapping of a cytokeratin 18 neo-epitope exposed during early apoptosis. J Pathol 187: 567–572.

Li H, Liu L, David ML, Whitehead CM, Chen M, Fetter JR, Sperl GJ, Pamukcu R, Thompson WJ. 2002. Pro-apoptotic actions of exisulind and CP461 in SW480 colon tumor cells involve beta-catenin and cyclin D1 down-regulation. Biochem Pharmacol 64:1325–1336.

Lin CS, Lau A, Tu R, Lue TF. 2000a. Identification of three alternative first exons and an intronic promoter of human *PDE5A* gene. Biochem Biophys Res Commun 268:596–602.

Lin CS, Lau A, Tu R, Lue TF. 2000b. Expression of three isoforms of cGMP-binding cGMP-specific phosphodiesterase (PDE5) in human penile cavernosum. Biochem Biophys Res Commun 268:628–635.

Liu L, Underwood T, Li H, Pamukcu R, Thompson WJ. 2002. Specific cGMP binding by the cGMP binding domains of cGMP-binding cGMP specific phosphodiesterase. Cell Signal 14:45–51.

MacKenzie SJ, Yarwood SJ, Peden AH, Bolger GB, Vernon RG, Houslay MD. 1998. Stimulation of p70S6 kinase via a growth hormone-controlled phosphatidylinositol 3-kinase pathway leads to the activation of a PDE4A cyclic AMP-specific phosphodiesterase in 3T3-F442A preadipocytes. Proc Natl Acad Sci USA 95:3549–3554.

Moon E-Y, Lerner A. 2002. Benzylamide sulindac analogues induce changes in cell shape, loss of microtubules and G_2–M arrest in a chronic lymphocytic leukemia (CLL) cell line and apoptosis in primary CLL cells. Cancer Res 62:5711–5719.

Morin PJ, Sparks AB, Korinek V, Barker N, Clevers H, Vogelstein B, Kinzler KW. 1997. Activation of β-catenin-Tcf signaling in colon cancer by mutations in β-catenin or APC. Science 275:1787–1790.

Piazza GA, Xu S, Klein-Szanto AJ, Ahnen DJ, Li H, Liu L, David M, Pamukcu R, Thompson WJ. 2000. Overexpression of cGMP phosphodiesterase (cG PDE) in colonic neoplasias compare to normal mucosa. Gastroenterology 118:1590.

Piazza GA, Thompson WJ, Pamukcu R, Alila HW, Whitehead CM, Liu L, Fetter JR, Gresh WE, Jr., Klein-Szanto AJ, Farnell DR, Eto I, Grubbs CJ. 2001. Exisulind, a novel proapoptotic drug, inhibits rat urinary bladder tumorigenesis. Cancer Res 61:3961–3968.

Pitari GM, Di Guglielmo MD, Park J, Schulz S, Waldman SA. 2001. Guanylyl cyclase C agonists regulate progression through the cell cycle of human colon carcinoma cells. Proc Natl Acad Sci USA 98:7846–7851.

Rybalkin SD, Rybalkina I, Beavo JA, Bornfeldt KE. 2002. Cyclic nucleotide phosphodiesterase 1C promotes human arterial smooth muscle cell proliferation. Circ Res 90: 151–157.

Sarfati M, Mateo V, Baudet S, Rubio M, Fernandez C, Davi F, Binet JL, Delic J, Merle-Beral H. 2003. Sildenafil and vardenafil, type 5 and 6 phosphodiesterase inhibitors, induce caspase-dependent apoptosis of B-chronic lymphocytic leukemia cells. Blood 101:265–269.

Schmidt M, Lu Y, Parant JM, Lozano G, Bacher G, Beckers T, Fan Z. 2001. Differential roles of $p21^{Waf1}$ and $p27^{Kip1}$ in modulating chemosensitivity and their possible application in drug discovery studies. Mol Pharmacol 60:900–906.

Schreiber M, Muller WJ, Singh G, Graham FL. 1999. Comparison of the effectiveness of adenovirus vectors expressing cyclin kinase inhibitors $p16^{INK4A}$, $p18^{INK4C}$, $p19^{INK4D}$, $p21^{WAF1/CIP1}$, and $p27^{KIP1}$ in inducing cell cycle arrest, apoptosis and inhibition of tumorigenicity. Oncogene 18:1663–1676.

Shailubhai K, Yu HH, Karunanandaa K, Wang JY, Eber SL, Wang Y, Joo NS, Kim HD, Miedema BW, Abbas SZ, Boddupalli SS, Currie MG, Forte LR. 2000. Uroguanylin treatment suppresses polyp formation in the Apc(Min/+) mouse and induces apoptosis in human colon adenocarcinoma cells via cyclic GMP. Cancer Res 60:5151–5157.

Soderling SH, Beavo JA. 2000. Regulation of cAMP and cGMP signaling: New phosphodiesterases and new functions. Curr Opin Cell Biol 12:174–179.

Soh J-W, Mao Y, Kim M-G, Pamukcu R, Li H, Piazza GA, Thompson WJ, Weinstein IB. 2000. Cyclic GMP mediates apoptosis induced by sulindac derivatives via activation of c-Jun NH2-terminal kinase. Clin Cancer Res 6:4136–4141.

Soh J-W, Mao Y, Liu L, Thompson WJ, Pamukcu R, Weinstein IB. 2001. Protein kinase G activates the JNK1 pathway via phosphorylation of MEKK1. J Biol Chem 276:16406–16410.

Sun W, Stevenson JP, Gallo JM, Redlinger M, Haller D, Algazy K, Giantonio B, Alila H, O'Dwyer PJ. 2002. Phase I and pharmacokinetic trial of the proapoptotic sulindac analog CP-461 in patients with advanced cancer. Clin Cancer Res 8:3100–3104.

Thompson WJ, Terasaki WL, Epstein PM, Strada SJ. 1979. Assay of cyclic nucleotide phosphodiesterase and resolution of multiple molecular forms of the enzyme. Adv Cyclic Nucleotide Res 10:69–92.

Thompson WJ, Piazza GA, Li H, Liu L, Fetter J, Zhu B, Sperl G, Ahnen D, Pamukcu R. 2000. Exisulind induction of apoptosis involves guanosine 3′,5′-cyclic monophosphate phosphodiesterase inhibition, protein kinase G activation, and attenuated β-catenin. Cancer Res 60: 3338–3342.

Thompson WJ, Ashikaga T, Kelly JJ, Liu L, Zhu B, Vemavarapu L, Strada SJ. 2002. Regulation of cyclic AMP in rat pulmonary microvascular endothelial cells by rolipram-sensitive cyclic AMP phosphodiesterase (PDE4). Biochem Pharmacol 63:797–807.

Tobey RA, Valdez JG, Crissman HA. 1988. Synchronization of human diploid fibroblasts at multiple stages of the cell cycle. Exp Cell Res 179:400–416.

Whitehead CM, Earle KA, Fetter J, Xu S, Hartman T, Chan DC, Zhao TL, Piazza G, Klein-Szanto AJ, Pamukcu R, Alila H, Bunn PA, Thompson WJ. 2003. Exisulind-induced apoptosis in a non-small cell lung cancer orthotopic lung tumor model augments docetaxel treatment and contributes to increased survival. Mol Cancer Ther 2:479–488.

Wu CF, Bishopric NH, Pratt RE. 1997. Atrial natriuretic peptide induces apoptosis in neonatal rat cardiac myocytes. J Bio Chem 272:14860–14866.

Xiong Y, Hannon GJ, Zhang H, Casso D, Kobayashi R, Beach D. 1993. p21 is a universal inhibitor of cyclin kinases. Nature 366:701–704.

Yoon J-T, Palazzo AF, Xiao D, Delohery TM, Warburton PE, Bruce JN, Thompson WJ, Sperl G, Whitehead C, Fetter J, Pamukcu R, Gundersen GG, Weinstein IB. 2002. CP248, a derivative of exisulind, causes growth inhibition, mitotic arrest, and abnormalities in microtubule polymerization in glioma cells. Mol Cancer Ther 1:393–404.